RC 21807 (98150) 25 July 2000 **Engineering and Technology**

IBM Research Report

TrueTrack Servo Technology for High TPI Disk Drives

Sri M. Sri-Jayantha, Hien Dang, Arun Sharma
IBM T. J. Watson Research Center
P. O. Box 218
Yorktown Heights, NY 10598

Isao Yoneda, Nabuyuki Kitazaki, Satoshi Yamamoto
IBM Japan Ltd.
Fujisawa-shi, Japan

Research Division
Almaden - Austin - Beijing - Haifa - T. J. Watson - Tokyo - Zurich

TrueTrack™ Servo Technology for High TPI Disk Drives

Sri M. Sri-Jayantha, IEEE Member
Hien Dang, Arun Sharma
IBM Research, Yorktown Heights, NY 10598, USA

Isao Yoneda, Nabuyuki Kitazaki, Satoshi Yamamoto
IBM Japan Ltd., Fujisawa-shi, Japan

Abstract

A disk drive with high track density faces positioning errors induced by disk shift, spindle vibration and disk warp. The spectrally rich error components are compensated for by high-gain digital filters. The filters augment the basic function of a conventional controller. Using a novel method fo initializing filters, precision tracking is achieved without compromising the settle out performance characteristics of a disk drive. The merit of cascade and parallel realization of the filters, both with a conventional servo controller, is considered. The effect of drift in amplitude and phase of the erro components is solved through an autonomous filter state propagation method during seek mode. A silicon servo chip is finally designed to incorporate the relevant functions of the algorithm.

I. Introduction

A novel servo algorithm to track complex head positioning errors is critical for a high TPI disk drive. Nominally, a track-following servo system is configured to provide precision within a fraction of a track width (a standard deviation of about 1/30th of track pitch). When stressed , for example unde vibration, a sustained data rate degradation of only 10% is tolerated by the customer. Hence, the challenge in the emerging high track density storage systems is to provide servo solutions to meet both nominal, as well as stressed, conditions without demanding costly components or abrupt change in the design of the disk drive.

The sources of head positioning errors can be categorized into various groups. Broadly considered, errors can be grouped into repeatable and non-repeatable components. Based on the spectral content of a position error signal (PES), the error sources can be grouped into harmonic, non-harmonic and broad band groups. For example, a disk shift is a narrow band harmonic, while PES noise is a broad band process. Subsequently, either a bandwidth-enhancing or a spectrally optimum servo solution to manage each error group becomes a natural objective. However, from a hard disk drive (HDD) viewpoint, under competitive access conditions, the transient dynamics of a head settle motion usually present a critical dilemma in finding an effective solution. Ultimately, a successful precision track-following performance can be attained only when access time is not compromised.

The present generation of rotary actuator-based sub 2.5”, 2.5" and 3.5" HDDs are designed to operate in hand-held, notebook and desk-top/server environments respectively. Mobile products are occasionally subjected to severe shocks leading to disk shift and desk-top/server HDDs are frequently exposed to spindle-induced vibration as shown in Figure 1. Each application area, thus, has a unique customer requirement to meet. Regardless of the mechanism that generates

track-follow errors, it is highly desirable to develop a servo solution that will compensate for the hardware deficiencies faced by an HDD in actual operation. This paper focuses on solving the positioning error problem caused by:

- *disk shift*
- *spindle vibration, and*
- *disk warp*

while *preserving optimum settle out* performance. The core of the concept has been patented and this reference [1] forms the basis for the paper. Several other related ideas presented herewith are also covered by various patent applications. Furthermore a common servo architecture that would lead to a software programmable solution across a range of HDD form-factors is considered for implementation.

II. Disk shift, Spindle-Induced Self-Vibration and Disk warp

A. Disk shift

A notebook computer with an embedded 2.5" disk drive may be subjected to harsh non-operating shock conditions and moderate operating vibration conditions. In response, the storage industry has focused on ruggedizing the HDD [2]. A shock vector of about 800g/1ms applied in the plane of a disk platter can produce a mean *disk shift* of 10 um (400 microinch). For a 25 kTPI HDD this amount of disk shift is equivalent to 10 tracks. Notebooks returned by customers confirm that disk shift is a reality, and the economics of repair cost alone could justify a solution to this problem.

The amount of mechanical disk shift can be minimized by firmer clamping of the disk platters to the spindle hub-flange or by improving the friction coefficient between spacer rings separating the disk platters. These options, however, have limits and side effects. Thus, a complimentary solution to the problem of disk shift through servo innovation deserves consideration. Any eccentricity in the rotating media produces a harmonic error component in the PES produced by the read head element. Traditionally this is referred to as a runout component, and it occurs at the spindle rotational frequency. One crucial problem is that of precise track-following in the presence of substantial eccentricity without compromising the settle out time. In an HDD with numerous disk-platters and heads, the disk shift is expected to be of a different magnitude for each platter, and a low cost solution to this problem is desirable.

B. Spindle-Induced Self-Vibration

A 3.5” HDD in a desk-top computer may not typically get exposed to a strong non-operating shock as anticipated in a 2.5” HDD, but it may undergo rotational vibration due to its own spindle mass imbalance. For example, at 25 kTPI, a vibration motion of a track under a read/write head due to spindle-induced *self-vibration* of about 1 um (40 microinch) corresponds to one track pitch. Due to component tolerance and manufacturing variation, it is not possible to have a perfectly mass balanced system. Attempts to dynamically balance a disk drive in a manufacturing line may help reduce the severity of this problem, but will not eliminate it.

Since a computer chassis is fabricated from basic sheet metal, an HDD mounting location can not be guaranteed to be rigid. Even a moderately compliant mini-tower or a server-rack system can

prove to be detrimental to the performance of a high TPI HDD. The amplitude of vibration is correlated to system specifics, and a 1 um error is only an optimistic estimate. Recently OEM integrators and HDD design teams have become more aware of chassis-dependent vibration problem [3].

Qualification and ease of integration of 3.5" HDDs has become a factor in differentiating competitive products by OEM clients [4]. There is a limit to how far the mounting arrangement can be made rigid enough to support high TPI drives. Constrained layer damping and the use of other esoteric materials to construct the HDD housing are tempting design options, but may not be cost effective. While spindle-induced vibration is dominant in 3.5" HDDs, disk shift due to thermal cycling can also contribute to PES. This error component merges with the vibration-induced component, but the spectral feature tends to be different for each source.

C. Disk warp

As the form factor of HDDs contracts from 3.5 " to 2.5", 1.8" and 1.0" configurations, the disk platter thickness is also reduced. The glass substrates used in the disk platters tend to warp due to non-uniform reactions to mechanical stress. One stress factor that exaggerates the warp is the clamp system design. The effect of warp is to produce primarily a Z-axis (spindle axis of rotation) dynamics of the slider. Similar to the effect seen in disk flutter mechanics, a vertical motion of the slider also gets translated into a fractional radial motion, thus resulting in a positioning error component. The warpage of a platter has been found to produce second and third harmonic radial position error components. Occasional encounters with even 6th harmonic during the developmental stage of an HDD is an indication of what is yet to come as higher TPI HDD design is envisaged.

The pivot hysteresis is suspected to interact with the disk shift driven actuator motion. Beyond a few microns the magnitude of head motion required to track a shifted disk could create higher harmonic disturbance torque arising from pivot non-linearity. Basic simulation study demonstrates a potential coupling mechanism as discussed at the end of this paper. Therefore multiple harmonic filters at large disk shift may be required to solve the non-linearity induced harmonics. The need for multiple filters is not solely attributable to disk warp.

III. Servo Requirement and Spectral Features

A head positioning servo system in an HDD performs three critical tasks. First, it moves the head to the vicinity of a target in a minimum time using a velocity servo under seek mode. Next, it positions the head on the target track with minimum transient using a settle out controller. Finally, the settle out controller changes to a proportional-integral-derivative (PID) type track follow controller. Literature that characterizes steady PES components can be found, for example [5]. The focus of this paper is to elaborate and solve the effect of a frequency-specific PES component resulting from disk shift, spindle-induced vibration or disk warp in an HDD.

The servo gain at the spindle frequency ought to have sufficient gain to reject a disk shift or self-vibration induced PES. Field experience shows that a conventional servo characteristics having about 20-40 dB gain at spindle fundamental harmonic frequency is not sufficient to meet the 3-sigma position error margin. To achieve a 10 % track pitch 3-sigma PES due to disk shift eccentricity (10 tracks), a rejection gain (=k) of 46 dB is required. This is computed as follows:

$$(10/k) = a \qquad (1)$$

where ‘a’ denotes the 0-pk sinusoidal amplitude (in track pitch unit) of the PES. The position error criteria corresponds to:

$$3x\ (a/2^{0.5}) < 0.1 \qquad (2)$$

Requirement (1) and (2) are satisfied when $k > 200$ (i.e., ~46 dB). Observe that the mechanical shift of a disk is bound to remain the same in absolute units for a given level of shock so that, as track density increases, the rejection requirement ought to increase proportionally. With ever increasing spindle rotational speed (RPM), achieving the same level of rejection at higher frequency can further complicate the servo requirements.

Harmonic errors due to disk shift, self-vibration, or disk warp are frequency specific, and the amplitude of the run out component tends to be stable when observed on a short time scale, i.e. in minutes. Bit a disk shift due to shock can be considered repeatable in the long term as it is affected by occasional shocks. A spindle-induced vibration component, on the other hand, is not long term repeatable as it is affected by mount compliance variation due to thermal fluctuations. The spectra characteristics of each component is different. The vibration component is due to dynamic coupling between spindle harmonic forcing function and mount compliance (kinetic) moderated by the HDD polar moment of inertia. Compared to this, the disk shift is simply a geometric (kinematics) imperfection occurring after a servo write operation. Thus, in the frequency domain, a disk shift would appear as a single narrow-band spectral component, but spindle-induced vibration appears with a peak having a finite bandwidth. Disks warp from outer diameter to inner diameter and may not take a pure sine-wave-like geometry - hence higher order harmonics sometimes become important for a true representation of the warp.

IV. Feed forward vs. Feedback Solution

Since the eccentricity or spindle-vibration induced PES occurs at a known frequency with a given amplitude, feed forward servo methods can be considered to reduce this error component. Feed forward methods assume that the actuator system has a well defined dynamic characteristics, so that the expected error component can be minimized by producing an actuator motion in anticipation of this error. However, the actuator system is known to contain plant parameters that are not predictable with confidence. For example, in the case of a rotary actuator system, the pivot bearings do not behave like an ideal bearing system and the friction in between sliding components becomes a source of uncertainty. Therefore, the feed forward methods are not robust and their consisten performance is not assured.

The method proposed in [6], for example, requires trigonometric manipulation of the PES in order to compute its Fourier components which, in turn, are used to generate the control signal. To counte errors seen in spectrally stable systems, a repetitive controller can be considered [7]. This solution addresses the steady state track-follow condition assuming a system with fixed parameters. To minimize the divergence in feed forward error due to parameter variation, an adaptive feed forward method using a repetitive controller is discussed in [8]. In a cost sensitive HDD it is desirable to search for a solution with minimum computational complexity so that less powerful microprocessors or custom logic can be employed.

According to [1], a robust feedback servo solution with optimum initial condition setup to operate a second order digital filter solves the disk shift problem with minimum settle out time penalty. The

simplicity of the solution and ease of product level integration has helped make the solution a standard in all IBM HDD products. A conceptually similar solution is pursued to manage the problem of spindle-induced vibration PES. Elements of TrueTrack™ servo technology are discussed below using an experimental example.

V. Essence of TrueTrack™ Servo Technology

Figure 2 shows a measured PES under a conventional servo due to a mechanically shifted disk platter. A digital servo controller receives a digitized PES and it generates a control signal after a series of multiply/add operation programmed into a control unit of an HDD. The run out componen at spindle rotation frequency appears as a dominant and persistent sinusoidal signal while nominal (i.e., the case with no disk shift) error components are superimposed onto it. Normal seek and settle out transient is followed by an attempt to track-follow, but the run out PES at spindle harmonic is clearly prevalent in this example. In this laboratory-based experiment, only a mild shock was applied to a 2.5" HDD in order to keep the eccentricity to a manageable level with a conventional servo.

Since the sinusoidal PES term due to disk shift corresponds to a fixed frequency component in the PES, application of a narrow-band/ high-gain digital filter to generate a high rejection gain at the corresponding frequency can be considered to be effective. Figure 3 shows the impact of a digital filter added in parallel to a conventional controller of Fig. 2 on the PES. The filter is activated at the end of a settle phase. During seek, the filter ought to be removed from undesirable excitation by the rapidly changing position error signal since the total head motion tend to be two-to-three orders of magnitude higher than that of a track-following motion. Hence the seek and early settle processes are executed with the filter removed from the servo loop. It can be seen from Fig. 3 that the high-gain filter enhances the steady PES value, but it takes about 15 to 20 ms to complete the attenuation of the disk shift error component. This characteristic of the solution is due to high-gain filter output having to evolve to a level commensurate with the input error against which the corrective control action is needed. Hence an intelligent method to eliminate the settle out transient, while preserving the steady state effectiveness of this solution, is in order. Note that in this example the filter state (shown schematically) tends to reach a steady oscillatory behavior, represented by its output, in about 3 to 4 cycles.

Observe that the filter state eventually reaches a steady oscillatory behavior and its discrete values corresponding to each servo sector can be stored in a RAM. The state value is correlated to the rotational position of a disk platter so that the sector number can be used as an address pointer to retrieve the stored state value. This *a priori* known state information can be exploited to minimize the settle out transient as discussed next. Figure 4 shows a second order digital filter realization (discussed in detail in the next section) in which the filter state M(n), M(n-1)... are stored in the control processor memory. Since the amount of disk shift is common to all tracks on a given platter only one sequence of the filter state is required to be stored and addressed as a function of sector number. By capturing the average value of the filter state during a power-ON initialization phase of an HDD, a representative value for the filter state is retained in the processor memory. Following a seek and a settle, the high-gain filter state (two elements M(n-1) and M(n-2)) is initialized using the stored state. The key effect of this step in the control algorithm is to remove the time it would take for the filter to reach its anticipated steady oscillatory value. The elegance of the solution is that the compensation effect is completely a feedback process rather than a feed forward process, but the initialization of the filter state is akin to a feed forward concept. The impact of this algorithmic solution is evident on the PES trace of Figure 4. Following a seek, the head is kept virtually on track with minimal or no perceptible transient dynamics.

VI. Servo Properties and Digital Filter Structure

The benefit of a high-gain digital filter augmenting a conventional servo controller has been demonstrated in the previous section. It is important to consider the effect of the filter on the conventional servo properties. The first question that comes to attention is that of servo stability. Figure 5 shows a computed openloop transfer function (OLTF) of a conventional servo and the effective OLTF with a high-gain filter located at 120 Hz (7200 rpm). This example is more appropriate for a 3.5" product, and the gain of the filter is exaggerated to provide an additional OLTF gain of 20 dB. The servo stability is preserved when the crossover frequency is kept substantially higher than the filter peak frequency. The filter bandwidth negatively impacts the phase of OLTF in the vicinity of the crossover region, and it specifically affects the *phase margin*. Hence, the filter bandwidth is gated by the loss in phase margin. Similar phase-based constraint is observed when multiple high-gain filters are employed to solve multiple harmonic components, as discussed later.

The structure of the digital filter must be selected for optimum realization of filter performance with the use of 16-bit integer arithmetic while supporting the VCM control in an HDD. In order to understand the impact of HDD parameters such as sampling rate, RPM, etc. it is useful to derive a closed form expression for the digital filter coefficients. This task is simplified by choosing an analog high-gain filter transfer function h(s) follows:

$$h(s) = P_a(s) / P_b(s) \qquad (3)$$

where

$P_a(s) = (s^2 + 2 \times \zeta_a \times \omega_a \times s + \omega_a^2)$

s = Laplace variable

$\omega_a = 2 \times \pi \times fa$

fa = undamped natural frequency corresponding to polynomial $P_a(s)$

ζ_a = damping ratio corresponding to polynomial $P_a(s)$

Using a bilinear transformation of the form

$$s = (2/T) \times (1-z^{-1}) / (1+z^{-1}) \qquad (4)$$

where 'z' is called the delay operator and 'T' is the sampling time, the analog transfer function can be transformed to a discrete form. Note that the frequency parameters *fa* and *fb* are related to a desired high-gain (peak) frequency f0. The simplest case is where *fa=fb=f0*. Once the transformation is completed, the new discrete transfer function equivalent is described as follows:

$$H(z) = [A + B z^{-1} + C z^{-2}] / [1 + E z^{-1} + F z^{-2}] \qquad (5)$$

For simplicity, a single delay operator z^{-1} is denoted as z1 and double delay operator z^{-2} is denoted as z2. It can be proved through substitution of eq. (4) into eq. (3) that the coefficients of eq. (5) are represented as follows:

Let fs = sampling frequency (Hz) (=1/T)

f* = f0/fs (Normalized peak frequency)

$$a1 = 2 x\pi \times \zeta_a \times f^*$$

$$a2 = (\pi \times f^*)^2 \quad (6)$$

$$b1 = 2 x\pi \times \zeta_b \times f^*$$

$$b2 = (\pi \times f^*)^2$$

then

$$D = [\ 1 + b1 + b2\ ]$$

$$A = [\ 1 + a1 + a2\ ] / D$$

$$B = [-2 +2 \times a2] / D \quad (7)$$

$$C = [\ 1 - a1 + a2\ ] / D$$

$$E = [-2 +2 \times b2] / D$$

$$F = [\ 1 - b1 + b2\ ] / D$$

The natural frequency for the numerator *(fa)* and denominator *(fb)* have been set equal to *f0*. Th second order filter of eq. (5) can be realized using different computational structures. Figure 6 shows a selective group of three structures. The obvious realization of eq. (5) corresponds to Structure -1 o Fig. 6 in which an intermediate variable Q(n) is introduced. A non-obvious version of the same filter is shown in Structure -2 with filter internal state defined as “R(n)”. Both forms are meant for cascade implementation with a conventional servo controller. Structure -3 of Fig. 6 corresponds to a bias free case where the filter internal state “M(n)” does not have to contain information about bias (or DC) value present in the input signal p(n). Furthermore, the filter Structure -3 shown inside the rectangl is the section that needs to be implemented in a parallel realization. Especially when the filter gain is high, the conventional servo controller design and
high-gain filter design process can be modularized and independently pursued.

VII. Parallel vs. Cascade Realization

Figure 7 shows a cascade realization of a multiple peak filter. The high-gain filters not only need to reduce the PES error at a desired frequency, but also ought to allow the free flow of control signals generated by the track-follow controller. This requirement imposes constraints on internal DC/AC gains and the numerical range corresponding to a structure of the filter. One could find elaborate discussions on optimum filter structures in literature on signal processing. An HDD-specific requirement is now discussed.

Internal DC gain of a filter structure determines the bias value of the filter state for a corresponding DC input. One key feature of the settle-out/track-follow control signal is to provide a bias command to the voice coil motor (VCM) driver so that the actuator can be placed at various track positions against the forces generated by the flexible cable, aerodynamic drag, and pivot hysteresis. Therefore, a cascade peak filter must allow the bias current command to remain continuous without any interruption, delay or, distortion during seek to settle mode switching. At minimum, the overal input/output DC gain must be unity when the filter is realized in cascade form. If this property is no preserved, transients in the settle out phase are introduced.

Since a filter's main function is to provide a salient compensating periodic control signal at a selected frequency, it can be expected to have a substantial amplitude on its output signal as well as on its internal state at this frequency. As it is a requirement to keep the fixed point arithmetic precision to a minimum number of bits in order to save silicon chip cost or MPU cost, it is necessary

to select a filter structure that will have not only a low internal DC gain, but also a moderate AC gain on its internal state without modifying the filter's input/output transfer function characteristics. Too high a gain can cause *numerical overflow* and too low a gain can cause *underflow*.

The estimation of filter gains at various internal stages is now made as a function of filter design parameters for each configuration shown in Fig. 6. Table. 1 summarizes the parametric DC gain of the filter at two internal stages. The first stage (Stage -1) is associated with input to internal state and the second stage (Stage -2) is associated with internal state to output. From Table -1 it is evident that internal DC gain for Structure -1 and - 2 is non-zero at both Stage -1 and Stage -2, whereas for the bias free realization of Structure -3 the internal gain is identically zero at Stage -2. Even more importantly, the internal gains are either directly or inversely proportional to the second power of the normalized frequency *(f*)* depending on the structure.

In Table -2 a numerical estimate of internal AC and DC gains for Stage -1 and Stage -2 are computed for a case when fs = 7920 Hz, f0=90 Hz. The example filter corresponds to a peak gain of 20 dB (ζ_a=0.08 and ζ_b =0.0058), and the respective filter coefficients are given as: A=1.0052, B=-1.9940, C=0.9938, D=1.0016, E=-1.9940, and F=0.9992. When the peak frequency is separated from the sampling frequency by about two orders of magnitude (i.e., f0= 90 Hz and fs = 7920 Hz), the internal DC gain can exceed 10^3 which is not a desirable condition for a 16-bit fixed point realization. In Structure -1 the Stage -1 DC & AC gains are low, but the Stage -2 gains are high, which may give rise to arithmetic underflow and potential computational quantization noise in the output stage. However, if the peak frequency and sampling frequency are kept within a factor of 10 to 20, the 16-bit implementation can be accommodated without concern in all these structures.

The ratio *(fs/f0)* significantly contributes to the internal gain values, and the greater the ratio the greater the internal gain values will be. If a bias current command is about 10 units, a filter with an internal gain, for example 2000 as in Structure -2, will have to reach an internal value of 20,000 bits in Stage -1 just to allow the DC value to pass through without distortion, thus resulting from internal arithmetic saturation or overflow. It was determined that such condition can be easily reached when the internal AC component is superimposed on the DC value. Figure 8 shows a developmental example of an HDD with a thermally shifted disk with an internal vibration component on which a cascade realization has been attempted. The bias level (DC) of the filter state is about 12,000 bits, and the AC component is about 7000 (0-pk).

Table - 1 Internal DC Gain of Each Filter Structure

Structure	Stage-1 Gain	Stage-2 Gain
1	$Q/p = 4 \times (pi \times f^*)^2 / D$	$Y/Q = D / [4 \times (pi \times f^*)^2]$
2	$R/p = D / [4 \times (pi \times f^*)^2]$	$Y/R = 4 \times (pi \times f^*)^2 / D$
3	$M/p = (A-1) / [4 \times (pi \times f^*)^2]$	V/M = 0

Table-2 AC/DC Gains for a 20 dB Peak Filter at f0=90 Hz & fs=7920 Hz.

Structure	Stage-1 DC Gain	AC Gain	Stage-2 DC Gain	AC Gain
1	Q/p = 0.005	= 0.0008	Y/Q = 1964.89	= 12240

2	R/p = 1964.89	= 12240	Y/R = 0.005	= 0.0008
3	M/p = 1.039	= 64.740	V/M = 0.0	= 0.141

Figure 9 shows a parallel realization of peak filters. Structure -3 is suitable for this implementation. The presence of (A-1) factor in Structure -3 in the DC Stage -1 gain moderates the maximum value. Therefore, in situations where sampling rates are forced to be high due to product design parameters or due to requirements of the chip design, then Structure -3 provides an optimum configuration. However, the factor (A-1) can become so low at high sampling rates that it can push the 16-bit numbers to less than a bit thus producing insensitivity at low signal levels. In order to provide protection against such a condition, other gain balanced structures can be further considered.

VIII. Parallel Realization for Spindle-Induced Vibration

There may be more than one drive mounted in a computer frame. Figure 10 shows an experimental set up with two dissimilar drives each generating a 75 Hz and 90 Hz spindle-induced vibration component respectively. Figure 11a , without a peak filter solution, confirms the vibration-induced PES of drive #A. For the purposes of demonstration, the spindle imbalances were artificially increased. Each drive is subject to self and *cross* vibration disturbances. By employing dual peak filters the PES signal for a drive can be enhanced in steady state as shown in Fig. 11b. In this paper the challenge of detecting the spindle RPM of a neighboring drive is not discussed. Even if the RPM is known, the next challenge is the addressing of the corresponding filter initial condition since for a given drive (say #A) the cross-vibration emanating from drive #B is not tightly phase coupled. Under this configuration, generating a proper address pointer to retrieve filter state value is not trivial. In Fig. 11c & d the filter initial condition is set to start from null value following a seek. Of course, the self-induced vibration filter can be initialized properly, allowing for partial optimality. The measured filter state data of Fig. 11b & 11c show the time domain behavior of the filter internal states. Each filter eventually reaches its own independent steady condition.

IX. Autonomous Filter State Generation

Several issues become evident when the full state value of a filter is required to be stored for future use as a string of binary numbers corresponding to each servo sector. When multiple platters are used the required storage space increases proportionally. When multiple filters are introduced, the storage requirement grows in multiples. These two issues can be resolved by either storing every other sample of the state and then reconstructing a lineally interpolated value, or their sinusoid-like wave form characteristics can be compressed into two binary words as an amplitude and phase information. Both solutions have been tested in the field and they are effective. However, more critical is the need to manage the effect of amplitude and phase drift of the PES on the filter state. Frequent updates of the filter state following a long track-follow operation is one option. A more elegant solution is discussed next.

Since the high-gain filters are lightly damped, the oscillatory nature of the filter dynamics is sustained even without a valid PES (in the case of parallel realization). Therefore, during a seek, instead of holding the filter computations, if the filter state is propagated *autonomously* continuing seamlessly from previous track-follow operation, there is an opportunity to estimate realistic filter state value in

the interim. Phase and amplitude continuity of the state in the autonomous mode is thus approximately maintained with simplicity. This solution is effective only when no head switch is required. Figure 12 is the autonomous filter operation in contrast to the case shown in Fig. 11. It can be observed that the settle out penalty is removed at the same time the filter states are conveniently projected forward. Whenever there is a head switch, the corresponding compressed state information must be retrieved to initiate the filter state for the first seek. From then on the same autonomous state propagation is pursued until another head switch is required.

X. Multiple-Harmonic Filters against Disk shift and Disk warp

In the previous section a configuration to use two parallel filters in a continuous mode was presented. At high track densities, disk shift and disk warp have been found to be significant in 2.5" and sub 2.5" form factor drives. In order to eliminate the PES error, a three-filter configuration corresponding to Fig. 9 is realized. The first, second, and third harmonic filters are used for this case. Fig. 13 compares the cases where the 2nd and 3rd harmonic filters have been initialized from zero in algorithm-1 and the autonomous mode has been used in the algorithm-2. The fundamental harmonic was initialized optimally from a table lookup for algorithm-1 and was constructed through autonomous operation for algorithm-2. Effectiveness in the settle out quality is observable between the two cases.

Finally, the question is: How does a customer perceive the value of TrueTrack™ servo solution? Figure 14 shows the impact of TrueTrack™ servo corresponding to the best mode realization shown in Fig. 13. In this example algorithm-1 is realized in a drive with lower track density than that containing algorithm-2. Therefore, at very low disk shift the single track seek time is slightly better for algorithm-1. As the disk shift level increases, the divergence between algorithm-1 and algorithm-2 solutions grows rapidly. The solution with autonomous mode shows almost no degradation in 1-track seek performance with disk-shifts of the order of 25 um. Fig.15 shows the impact on format unit time. This is a process where '0' is written on all the user data surfaces. It is clear that the autonomous mode shows only about 15% degradation at 28 um disk shift whereas the algorithm-1 design shows substantial degradation beyond 4 um disk shift.

The use of higher harmonic filters in the above example demonstrates the enhancement in performance. Nevertheless, the disturbance source could have been either disk warp or harmonics generated by pivot hysteresis. An early work done using a simulation scheme sheds some light. Figure 16a & b show two FFT spectrums under a disk shift (5 tracks 0-pk) without and with a fundamental harmonic filter. Even though a second and a third harmonic PES error sources were not included in the simulation, the PES specturm does show the presence of these components. Only pivot non-linearity was included in the simulation model. Figure 16b shows the attenuation of fundamental harmonic (at 60 Hz), but the other harmonics remain in the spectrum.

XI. Product Impact and High TPI Future Configurations

Since the high-gain peak filters have been very effective in solving the frequency specific PES problem, the solution has been now integrated into an LSI module. Fig.17 shows the IBM product coverage. Most of this information is covered in the IBM product brochures and website for the benefit of customers. Several million HDD units have been shipped with TrueTrack™ servo technology embedded in them.

As track density of an HDD continues to grow exponentially, new hardware and servo algorithms will come under intense scrutiny. Will there be a transition to a MEMS solution in the near future or will

there be innovations in multiple fronts on the present subsystems that will propel the storage technology further? Use of a frictionless pivot with a torque-generating actuator assembly [9-10] may be an alternative option. As servo bandwidth plateaus, hardware designs that may reduce rotational vibration coupling may become an important element in solving the high track density challenge. These topics will be discussed in our future publications.

XII. Conclusions

A novel algorithm has been demonstrated to compensate for frequency specific PES components without compromising the settle out performance in a disk drive environment. The PES components could result from either a disk shift, spindle-imbalance or disk warp. The algorithm consists of multiple second order digital high-gain filters optimally initialized following a settle out phase. The initialization process is shown to be replaceable by an autonomous filter state propagation method. A bias-free filter structure configured in parallel to a conventional servo is tested and shown to be the best mode realization of the TrueTrack™ servo method. A silicon servo chip has been now designed to incorporate these functions.

Acknowledgment

To the members of the IBM Fujisawa, Japan HDD development team: Y. Nakagawa, N. Kagami, T. Ueda, A. Tokizono, T. Sakai, M. Kisaka and Y. Ozawa, and to Avis Harrell Sri-Jayantha for proof reading.

References

[1] S. M. Sri-Jayantha, A. Sharma, H. Dang, and S. Yamamoto, “Robust servo for disk shift compensation in rotating storage system,” U.S. Patent 5,608,586, Mar. 4, 1997.

[2] S. M. Sri-Jayantha, V. Khanna, S. Kumar, H. Dang, A. Sharma, K. Takahashi, H. Matsuda and I Yoneda, “Designing hard drives to withstand hard knocks,” Data Storage, pp.37-40, Oct., 1998.

[3] M. Suwa and K. Aruga, “Evaluation System for Residual Vibration from HDD Mounting Mechanism,” IEEE Transaction on Magnetic, Vol. 35, No. 2, pp. 868-873, Mar. 1999.

[4] http://www.storage.ibm.com/hardsoft/diskdrdl/technolo/truetrack.htm (also do a search for *truetrack* in the website www.storage.ibm.com)

[5] R. Ehrlich and D. Curran, “Major HDD TMR Sources and Projected Scaling with TPI,” IEEE Transaction on Magnetic,” Vol. 35, No. 2, pp. 885-891, Mar. 1999.

[6] M. Sidman, “Adaptive misposition correcting method and apparatus for magentic disk servo system,” U.S. Patent 4,536,809, Aug. 20, 1985.

[7] M. Tomizuka, T.C. Tsao, and K. K. Chew, “Discrete-time domain analysis and synthesis of repetitive controllers, “ ASAME J. Dynamic Systems, Measurement and Control, Vol. 3, pp. 353-358, Sept. 1989.

[8] A. Sacks, M. Bodson and W.. Messner, “Advanced methods for repeatable run out compensation,” IEEE Transaction on Magnetic, Vol. 31, No. 2, pp. 1031-1036, Mar. 1995.

[9] S. M. Sri-Jayantha, A. Sharma, S. Kumar, and V. Khanna, “Direct access storage device having a compound actuator bearing system,” U.S. Patent 5,761,006, June 2, 1998.

[10] H. Ottesen and S. M. Sri-Jayantha, “Rotary actuator for a direct access storage device,” U.S. Patent 5,267,110, Nov. 30, 1993.

List of Figures:

.

High-TPI Challenges

- **Disk-Shift due to Shock**
- **Disk-Warp due to Stress**
- **Spindle Vibration due to Imbalance**

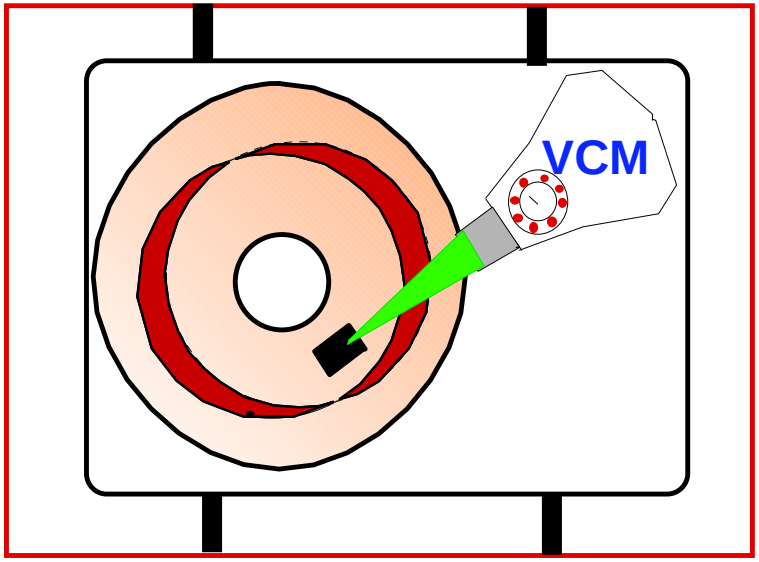

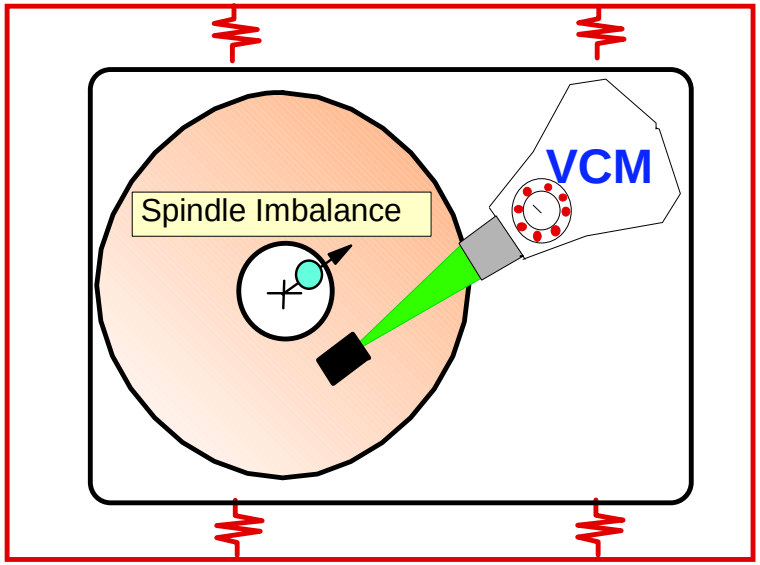

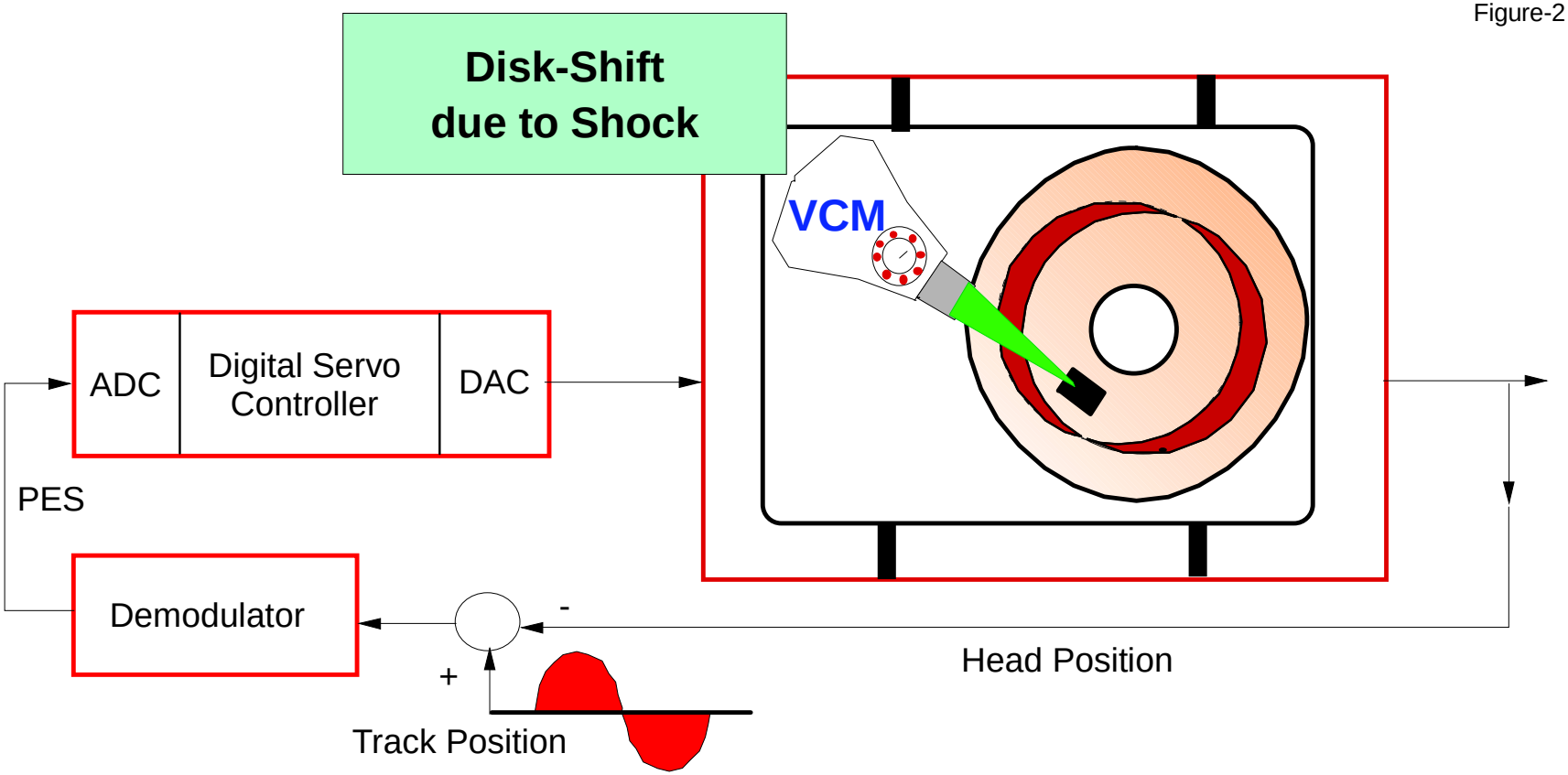
Disk-Shift
due to Shock
VCM
ADC
Digital Servo
Controller
DAC
PES
Demodulator
-
+
Head Position
Track Position

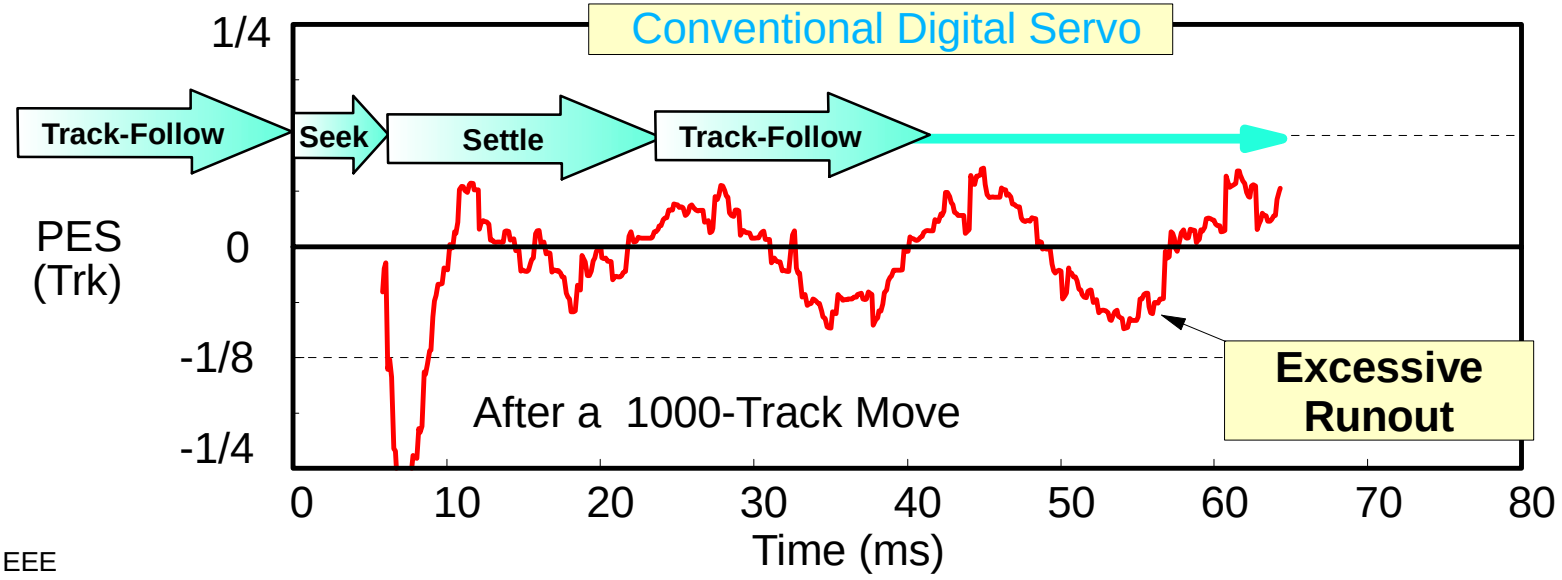
Conventional Digital Servo
1/4
Track-Follow
Seek
Settle
Track-Follow
PES
(Trk)
0
-1/8
-1/4
After a 1000-Track Move
Excessive
Runout
0
10
20
30
40
50
60
70
80
Time (ms)

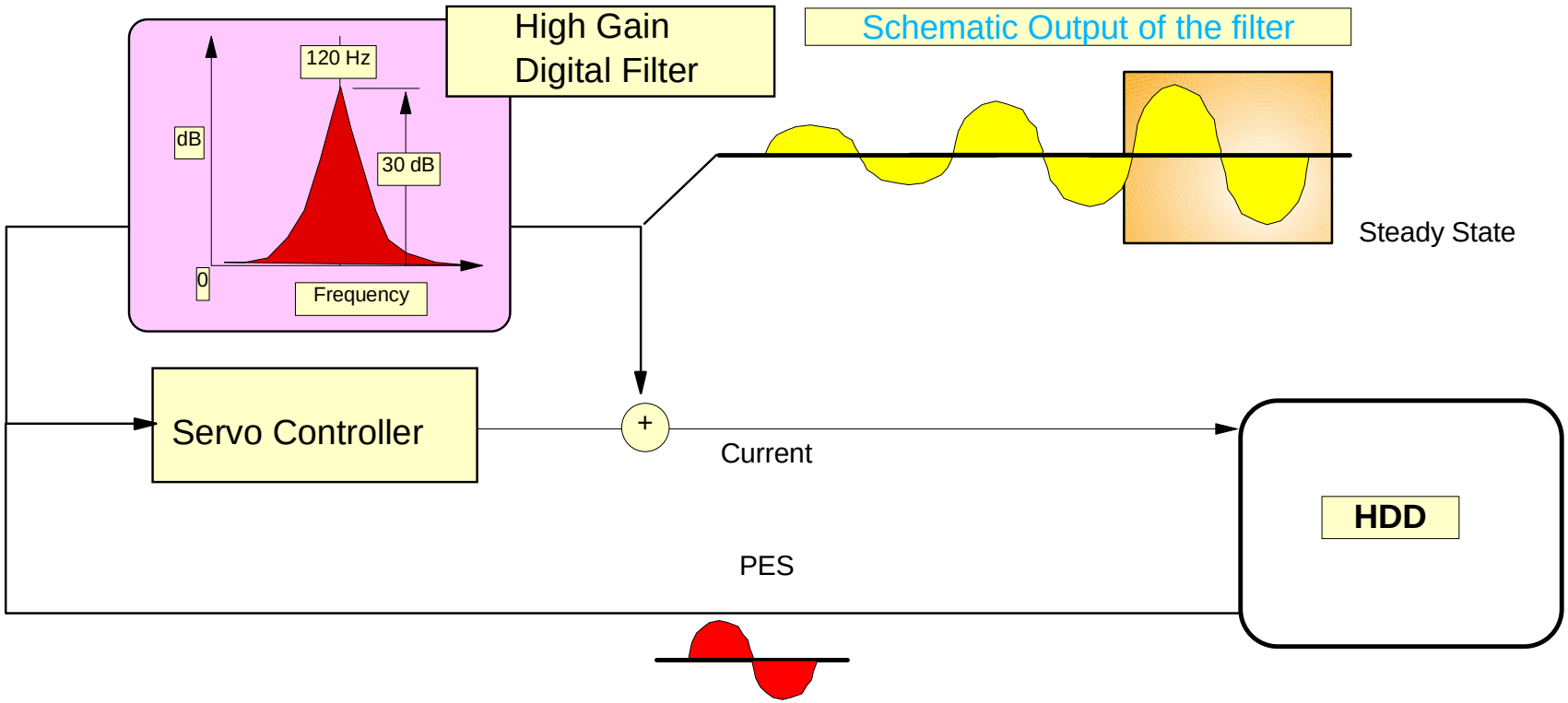
High Gain
Digital Filter
120 Hz
dB
30 dB
0
Frequency
Schematic Output of the filter
Steady State
Servo Controller
+
Current
HDD
PES

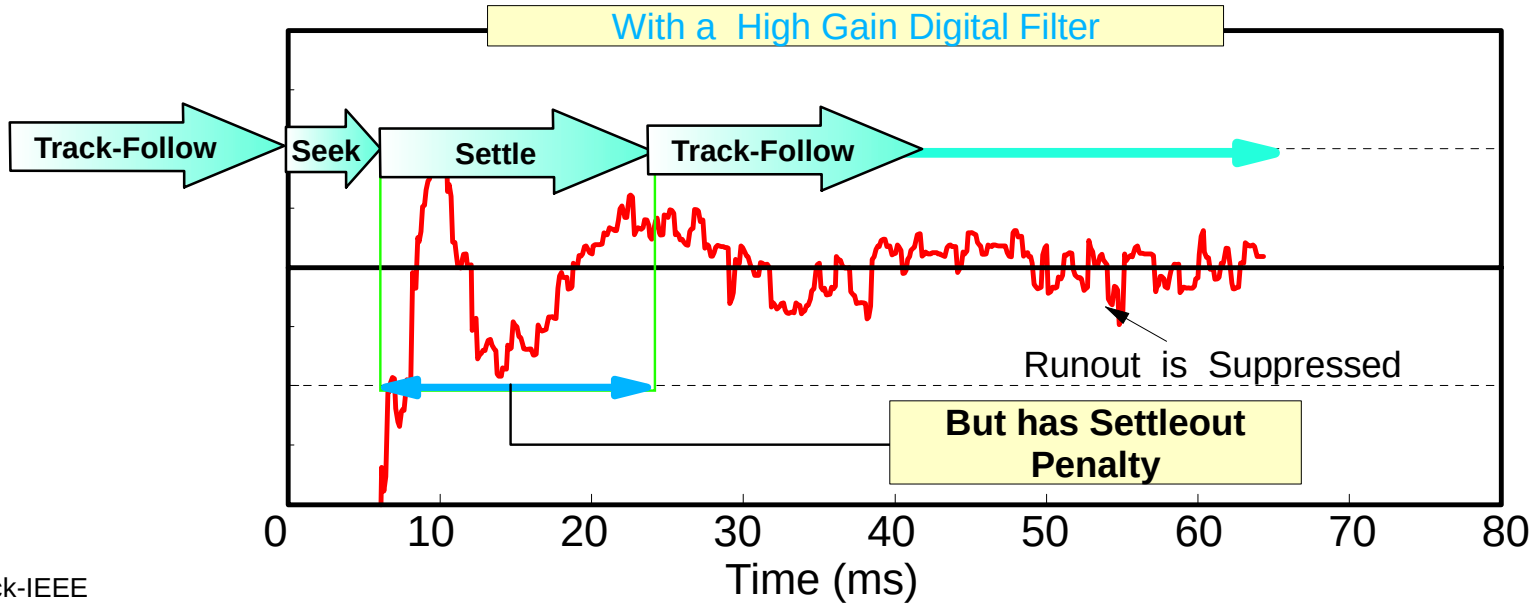
With a High Gain Digital Filter
Track-Follow
Seek
Settle
Track-Follow
Runout is Suppressed
But has Settleout
Penalty
0
10
20
30
40
50
60
70
80
Time (ms)

Figure-4

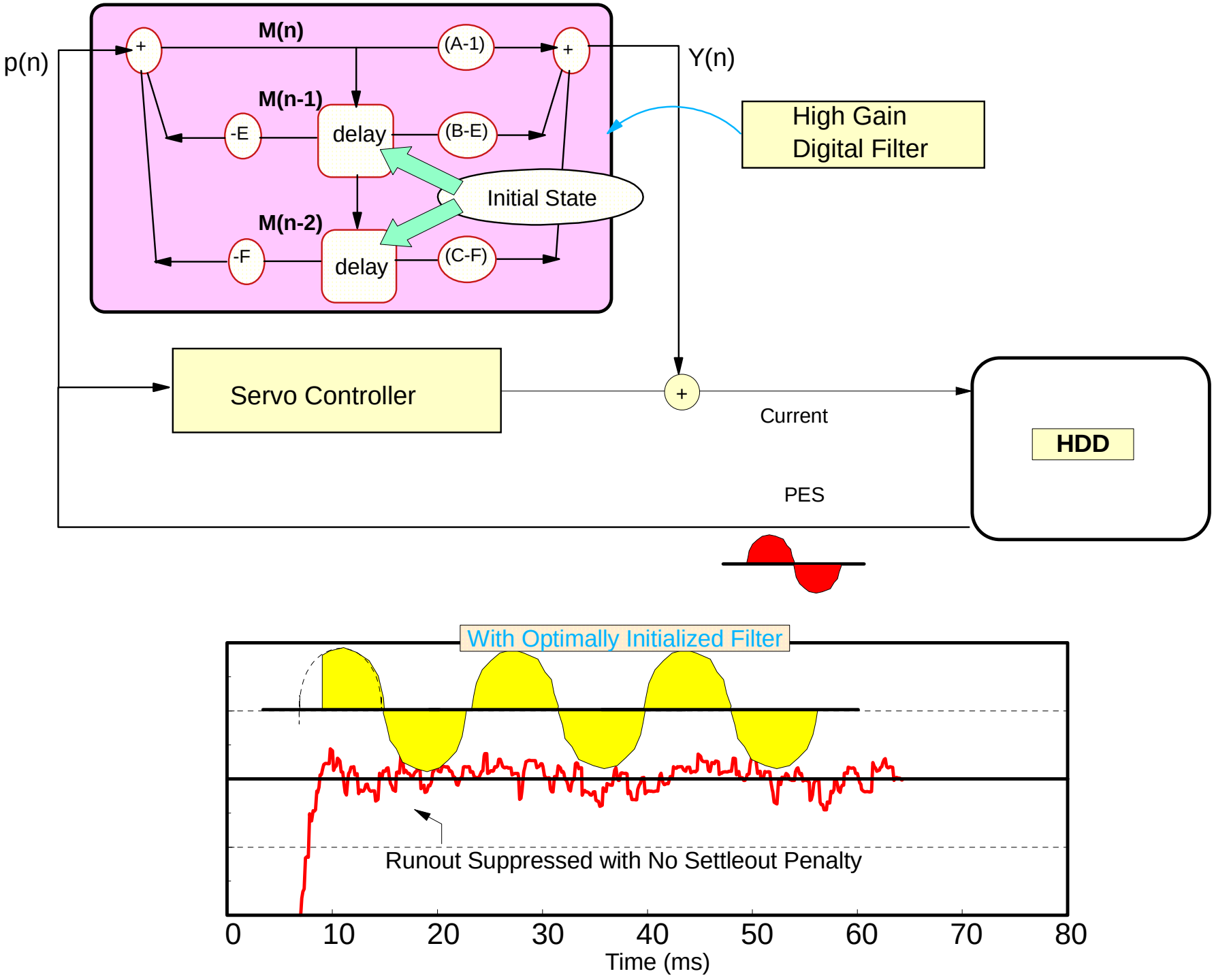
p(n)
M(n)
+
(A-1)
+
Y(n)
M(n-1)
-E
delay
(B-E)
High Gain
Digital Filter
Initial State
M(n-2)
-F
delay
(C-F)
Servo Controller
+
Current
HDD
PES
With Optimally Initialized Filter
Runout Suppressed with No Settleout Penalty
0
10
20
30
40
50
60
70
80
Time (ms)

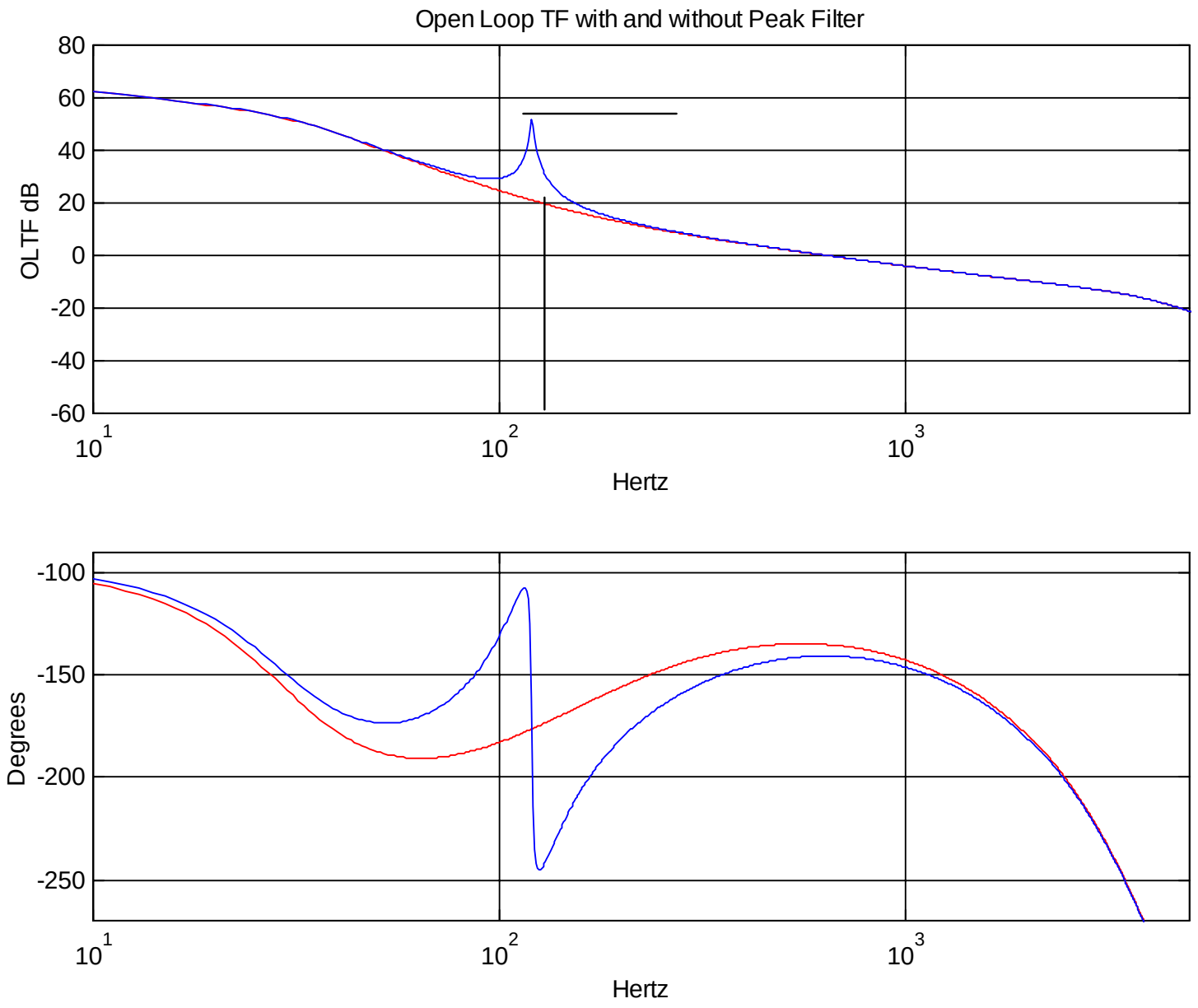
Open Loop TF with and without Peak Filter
80
60
40
20
0
-20
-40
-60
OLTF dB
10^1
10^2
10^3
Hertz
-100
-150
-200
-250
Degrees
10^1
10^2
10^3
Hertz

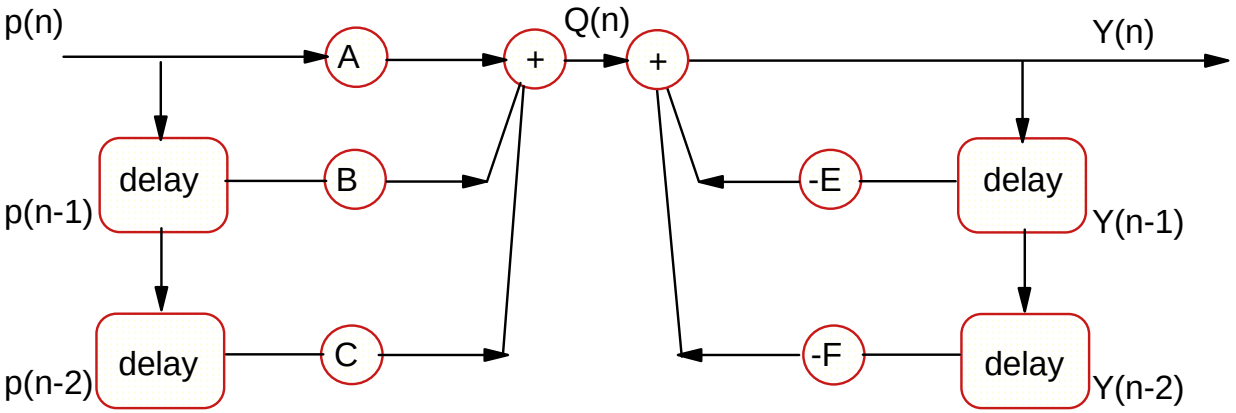

1

Y(n)=A p(n)+B p(n-1)+C p(n-2) - E Y(n-1) - F Y(n-2)

Direct-Form

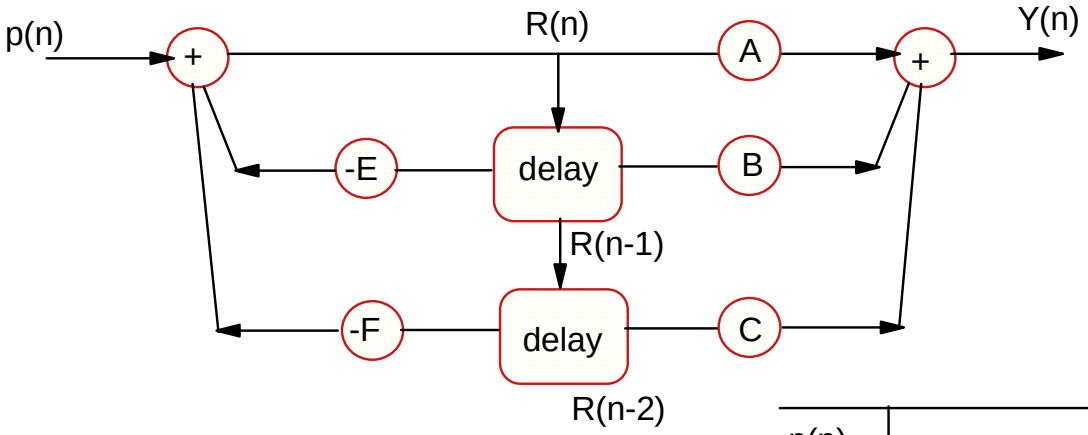

2

Bias Free Form

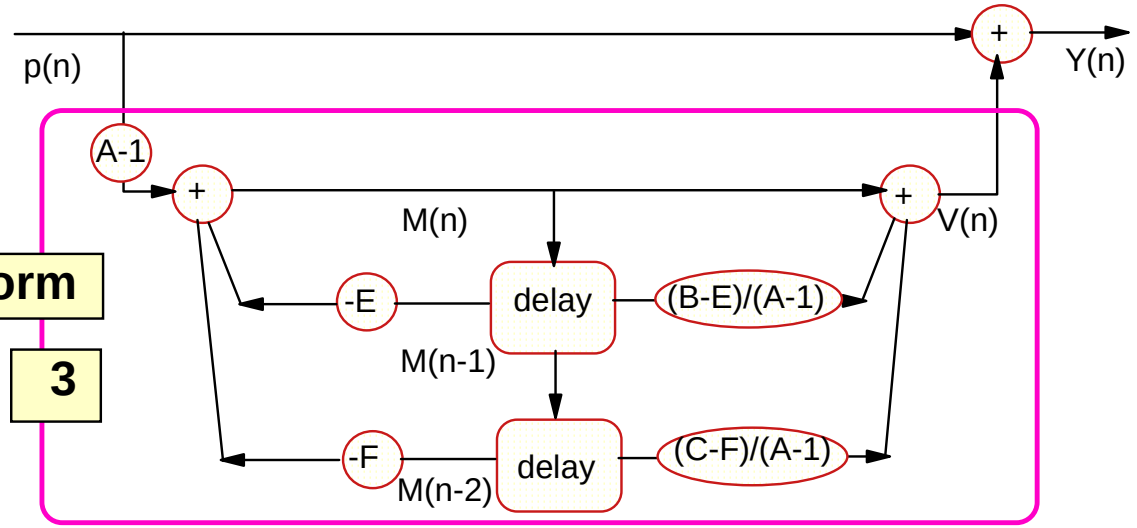

3

Figure-7

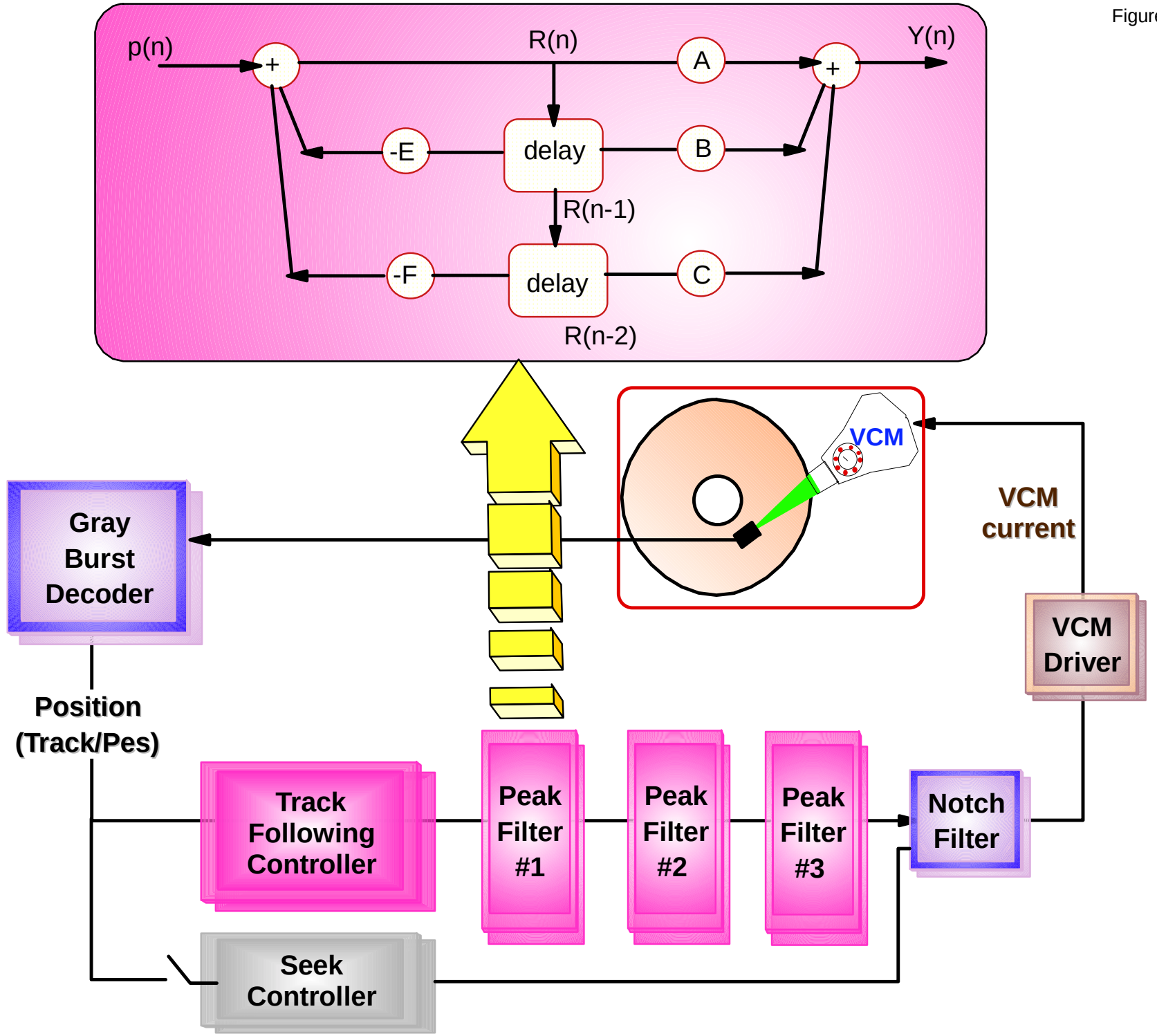
p(n)
+
R(n)
A
+
Y(n)
-E
delay
B
R(n-1)
-F
delay
C
R(n-2)
VCM
VCM current
Gray Burst Decoder
VCM Driver
Position (Track/Pes)
Track Following Controller
Peak Filter #1
Peak Filter #2
Peak Filter #3
Notch Filter
Seek Controller

Figure-8

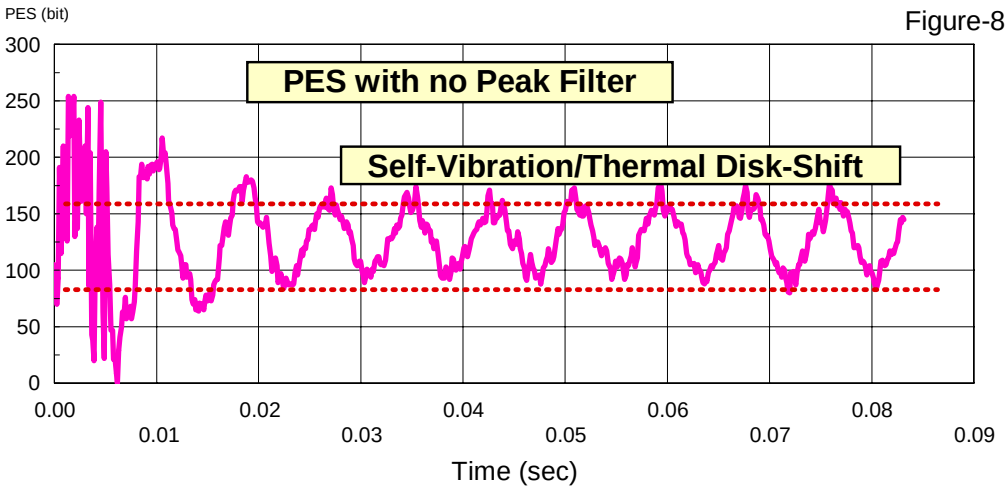
PES (bit)
PES with no Peak Filter
Self-Vibration/Thermal Disk-Shift
300
250
200
150
100
50
0
0.00
0.01
0.02
0.03
0.04
0.05
0.06
0.07
0.08
0.09
Time (sec)

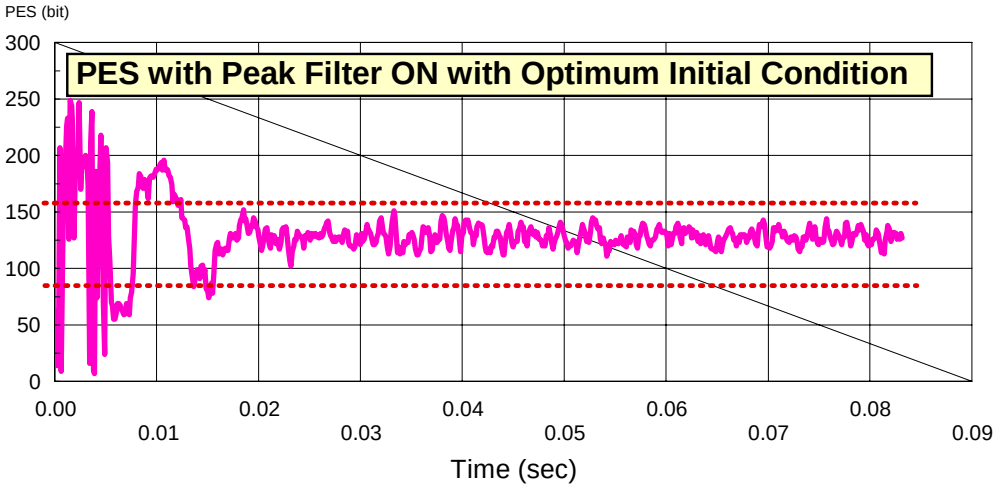
PES (bit)
PES with Peak Filter ON with Optimum Initial Condition
300
250
200
150
100
50
0
0.00
0.01
0.02
0.03
0.04
0.05
0.06
0.07
0.08
0.09
Time (sec)

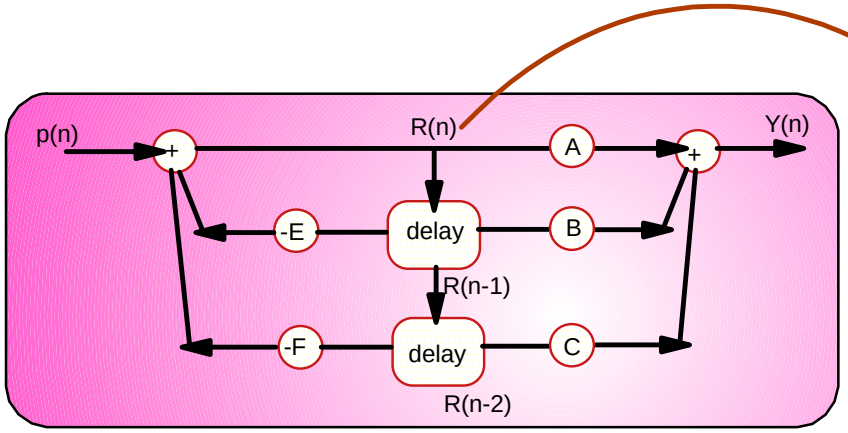
p(n)
R(n)
Y(n)
+
A
+
-E
delay
B
R(n-1)
-F
delay
C
R(n-2)

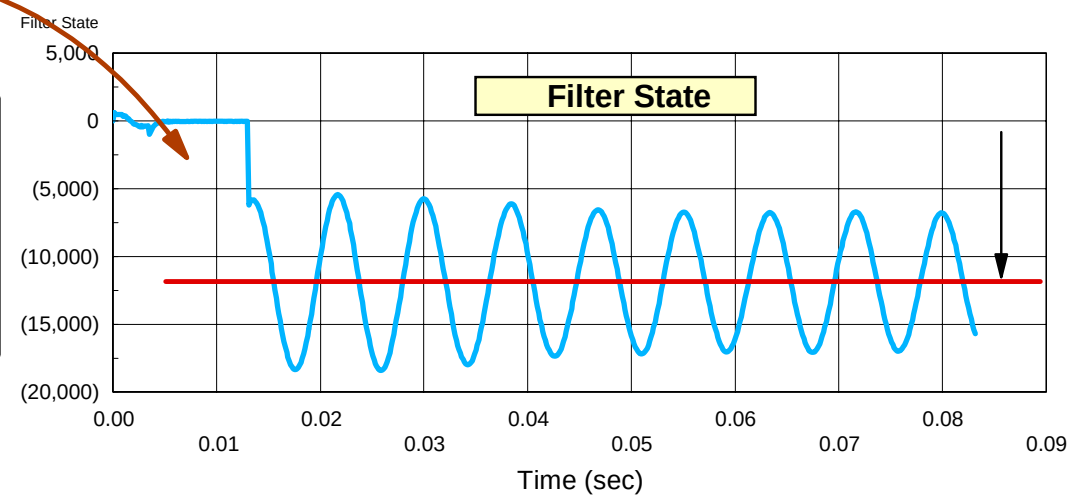
Filter State
Filter State
5,000
0
(5,000)
(10,000)
(15,000)
(20,000)
0.00
0.01
0.02
0.03
0.04
0.05
0.06
0.07
0.08
0.09
Time (sec)

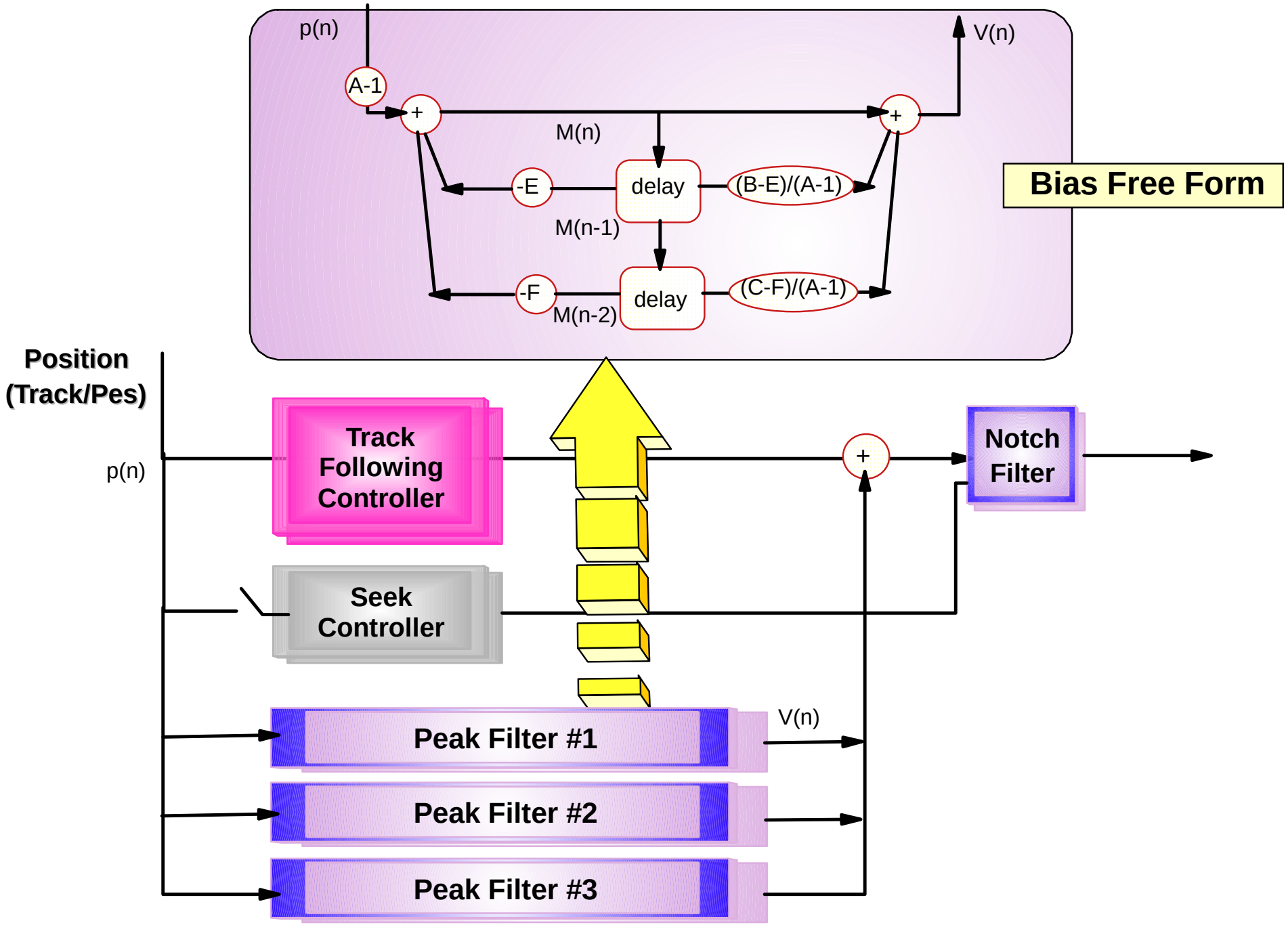
p(n)
A-1
+
M(n)
+
V(n)
-E
delay
(B-E)/(A-1)
M(n-1)
-F
delay
(C-F)/(A-1)
M(n-2)
Bias Free Form
Position
(Track/Pes)
p(n)
Track
Following
Controller
Seek
Controller
+
Notch
Filter
V(n)
Peak Filter #1
Peak Filter #2
Peak Filter #3

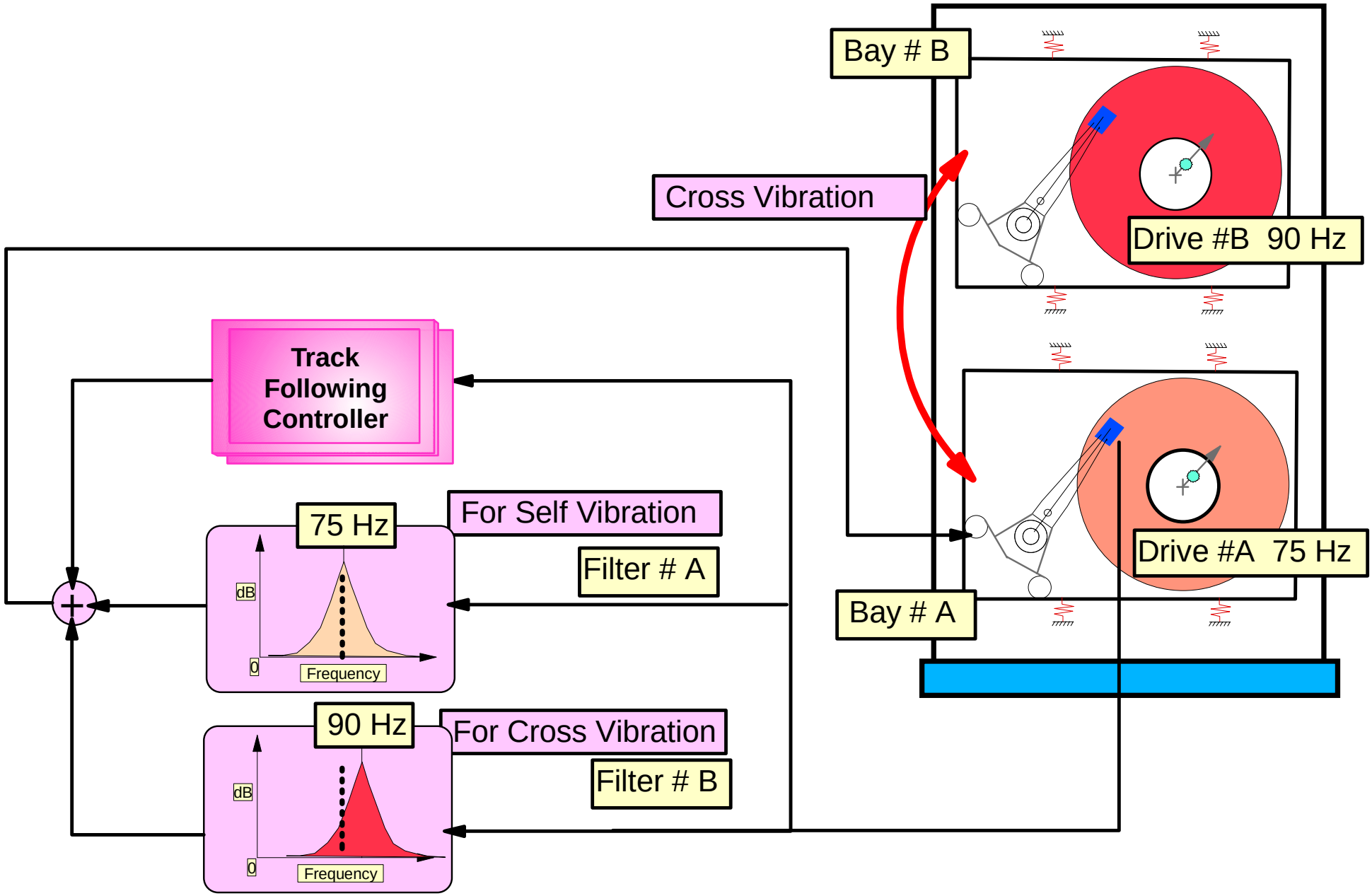
Bay # B
Cross Vibration
Drive #B 90 Hz
Track Following Controller
75 Hz
For Self Vibration
Filter # A
dB
0
Frequency
Drive #A 75 Hz
Bay # A
90 Hz
For Cross Vibration
Filter # B
dB
0
Frequency

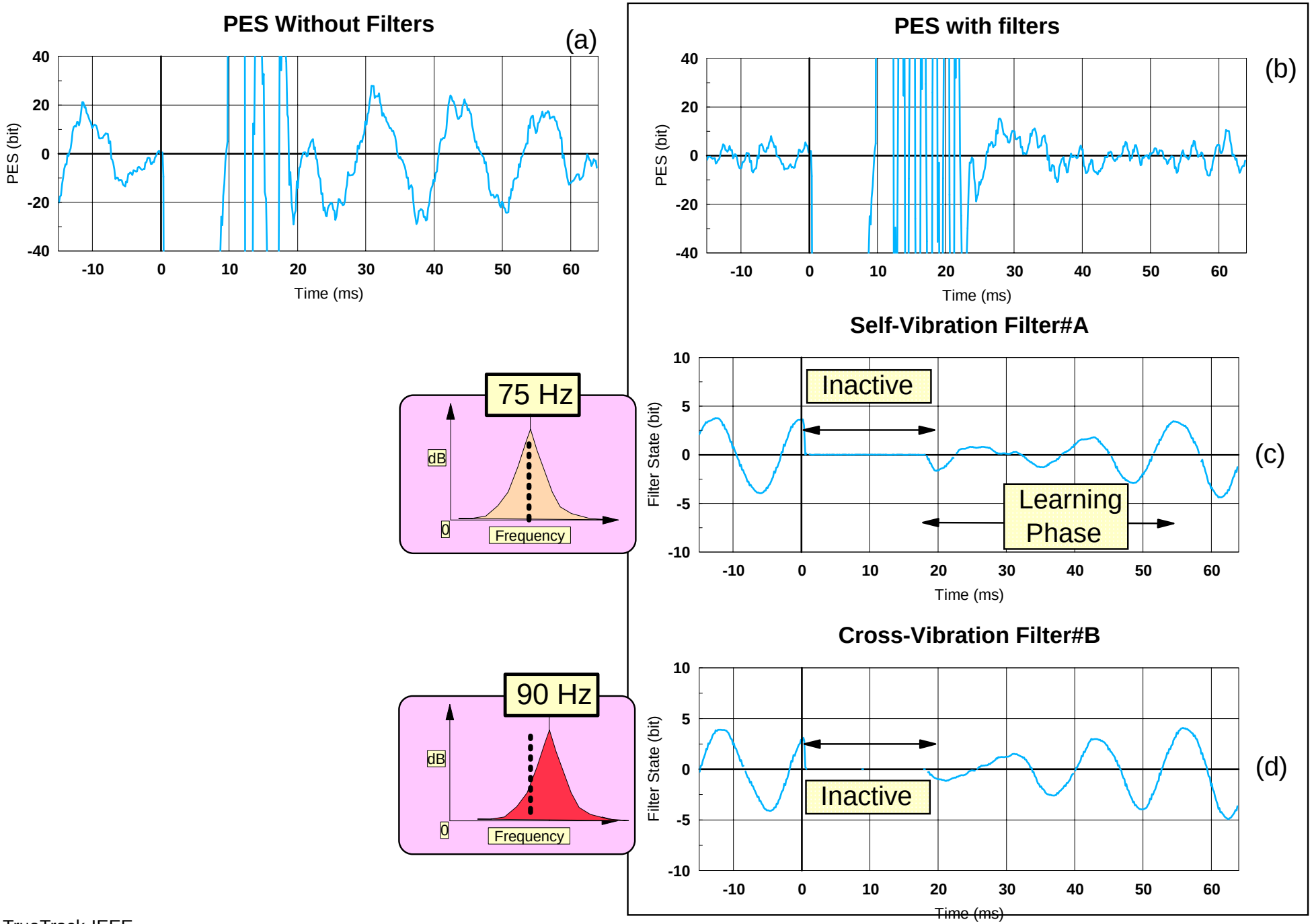
PES Without Filters
(a)
PES (bit)
Time (ms)
PES with filters
(b)
PES (bit)
Time (ms)
Self-Vibration Filter#A
75 Hz
dB
0
Frequency
Inactive
Learning
Phase
Filter State (bit)
Time (ms)
(c)
Cross-Vibration Filter#B
90 Hz
dB
0
Frequency
Inactive
Filter State (bit)
Time (ms)
(d)

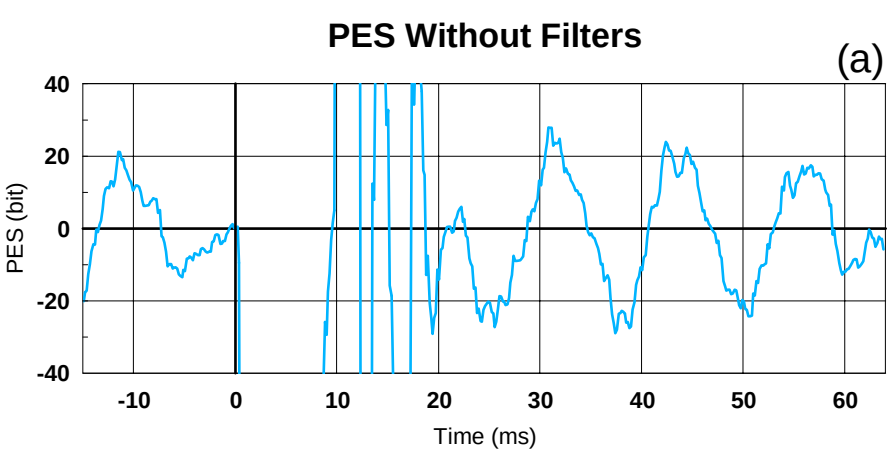
PES Without Filters
(a)
PES (bit)
Time (ms)

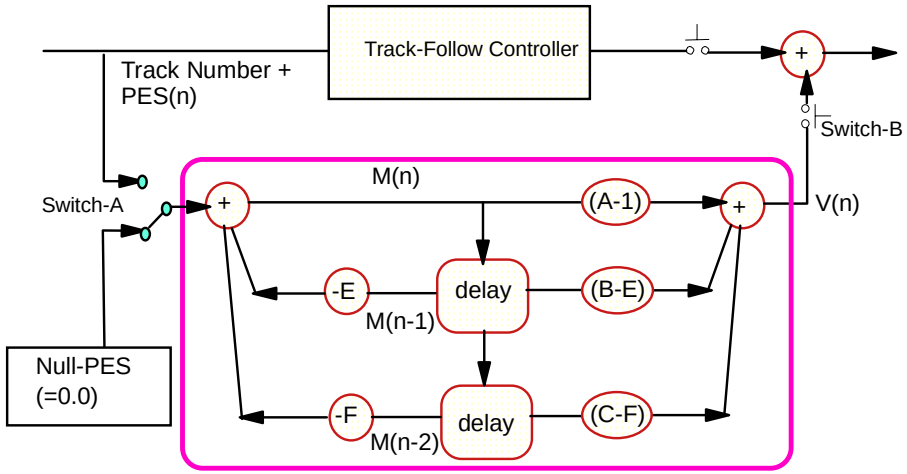
Track Number +
PES(n)
Track-Follow Controller
Switch-B
Switch-A
M(n)
(A-1)
V(n)
-E
delay
(B-E)
M(n-1)
Null-PES
(=0.0)
-F
delay
(C-F)
M(n-2)

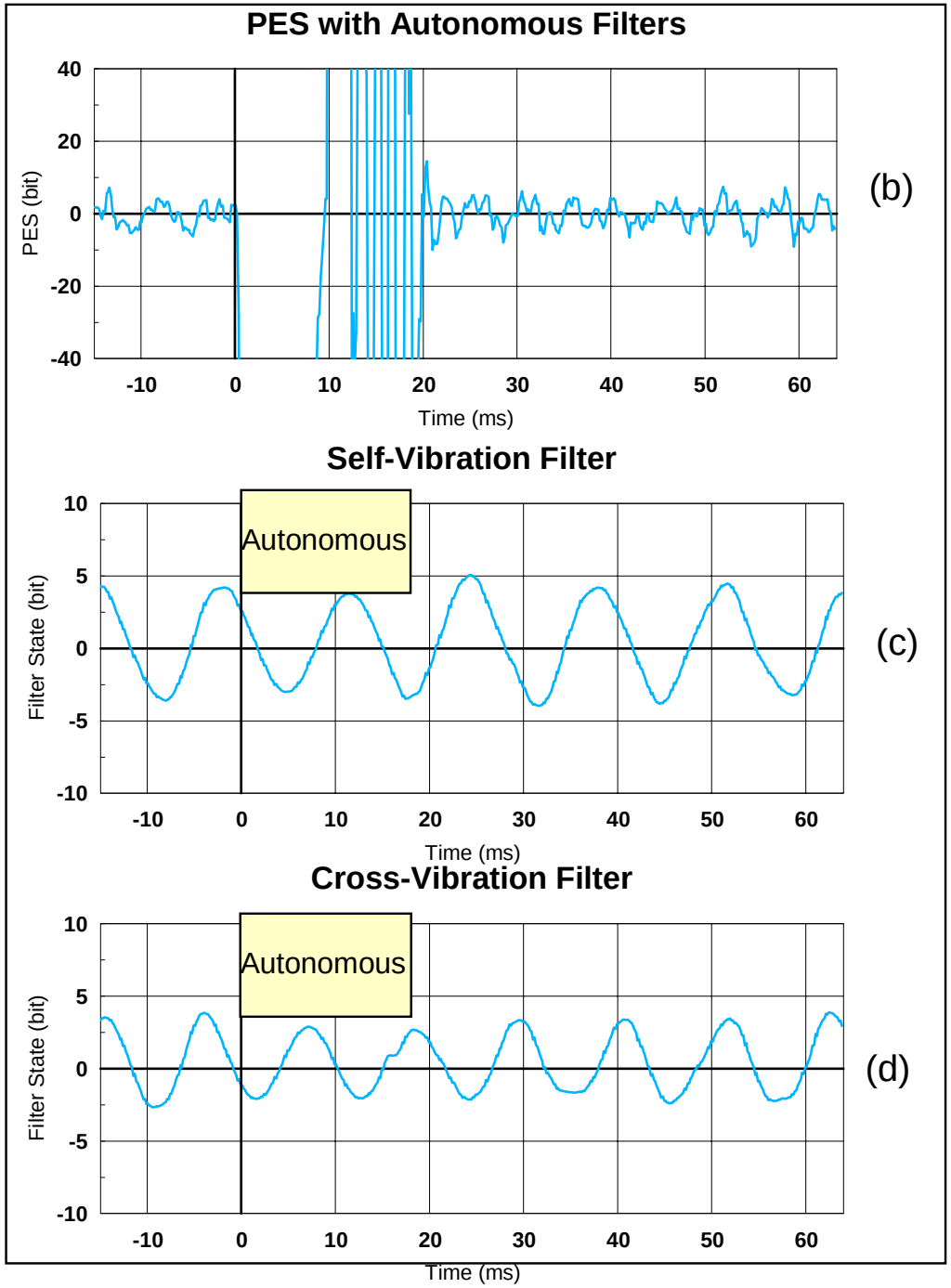
PES with Autonomous Filters
PES (bit)
Time (ms)
(b)
Self-Vibration Filter
Autonomous
Filter State (bit)
Time (ms)
(c)
Cross-Vibration Filter
Autonomous
Filter State (bit)
Time (ms)
(d)

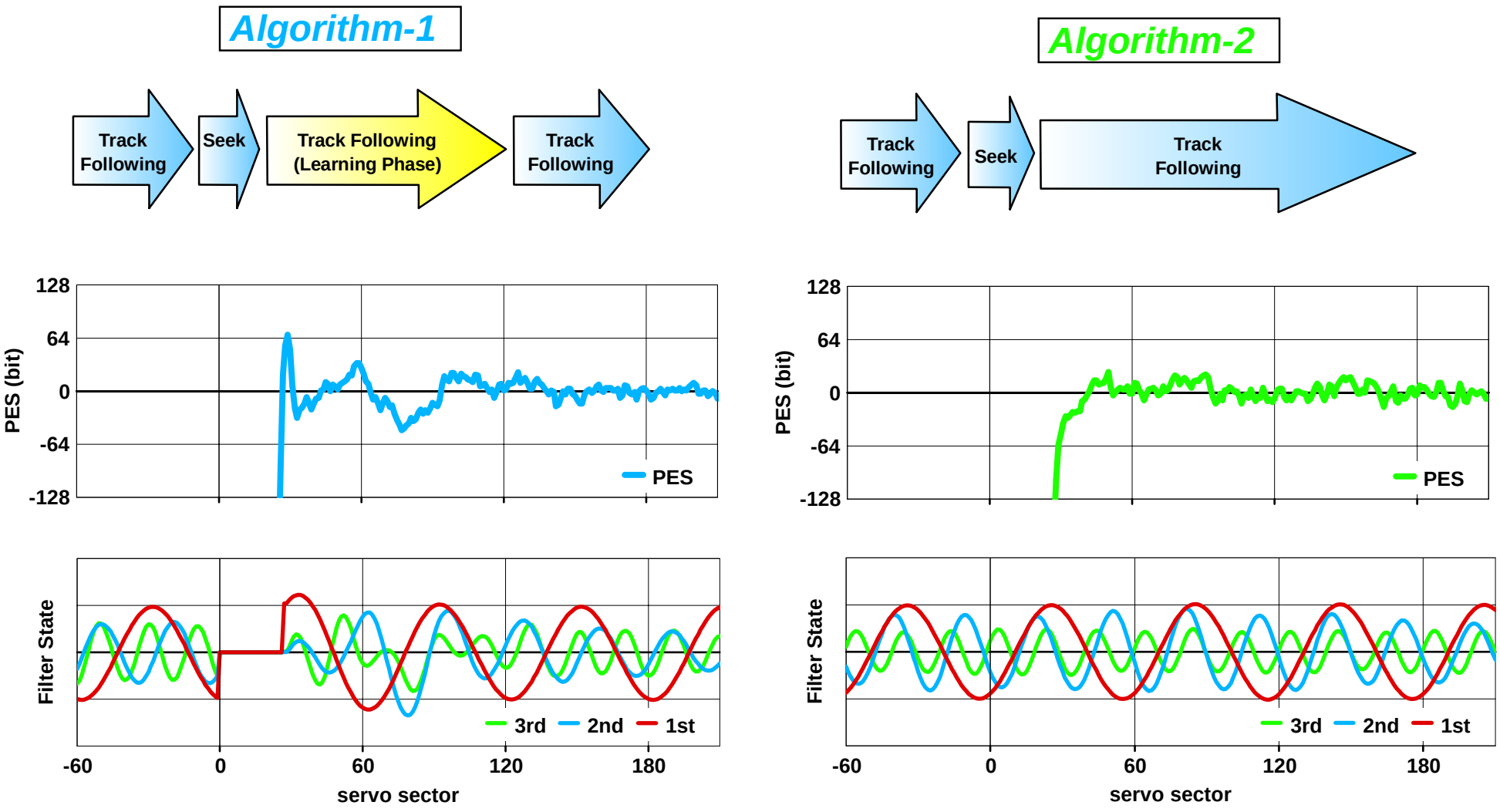
Algorithm-1
Track Following
Seek
Track Following (Learning Phase)
Track Following
Algorithm-2
Track Following
Seek
Track Following
128
64
0
-64
-128
PES (bit)
PES
Filter State
3rd
2nd
1st
-60
0
60
120
180
servo sector

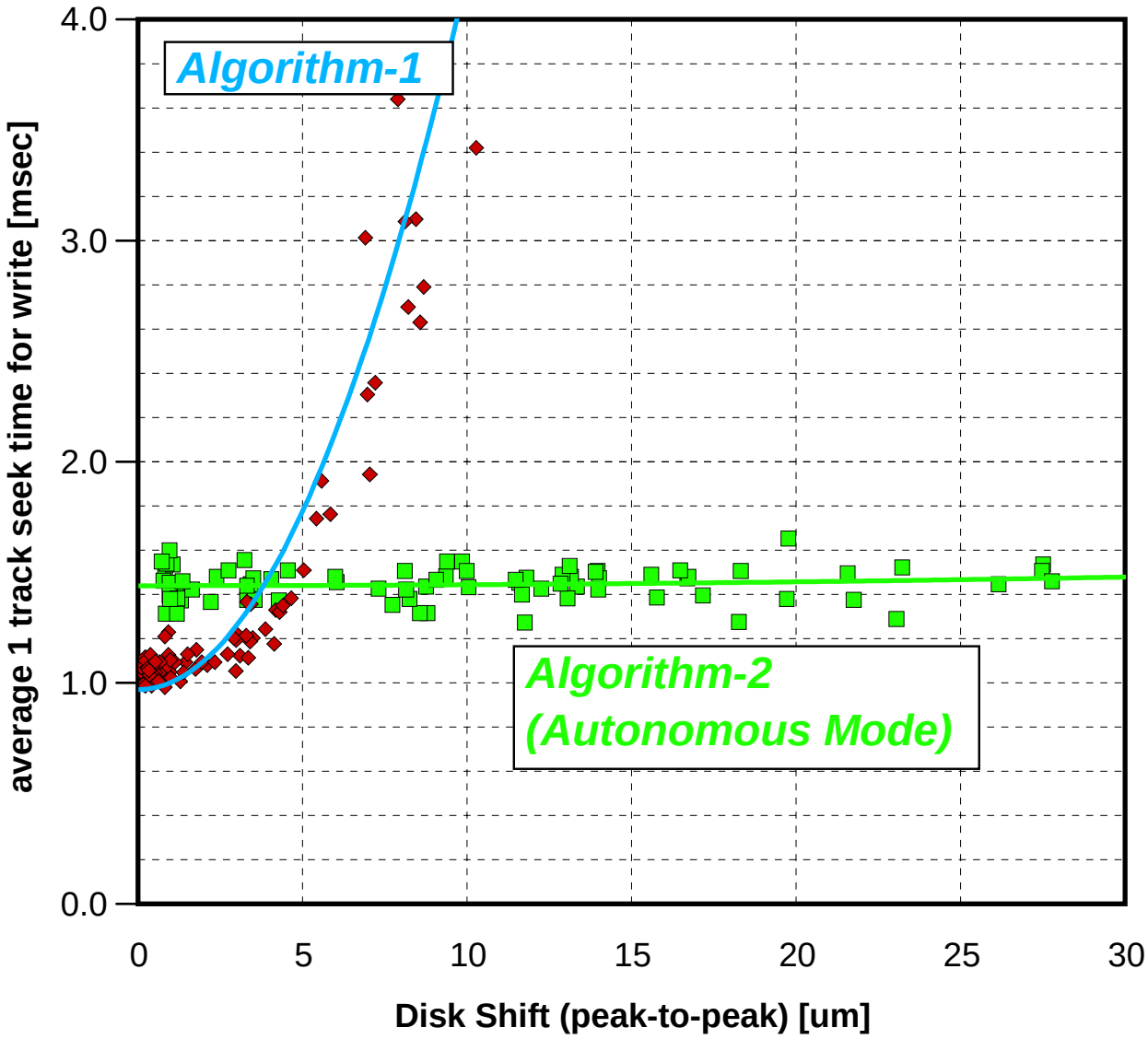
Algorithm-1
Algorithm-2
(Autonomous Mode)
average 1 track seek time for write [msec]
Disk Shift (peak-to-peak) [um]
4.0
3.0
2.0
1.0
0.0
0
5
10
15
20
25
30

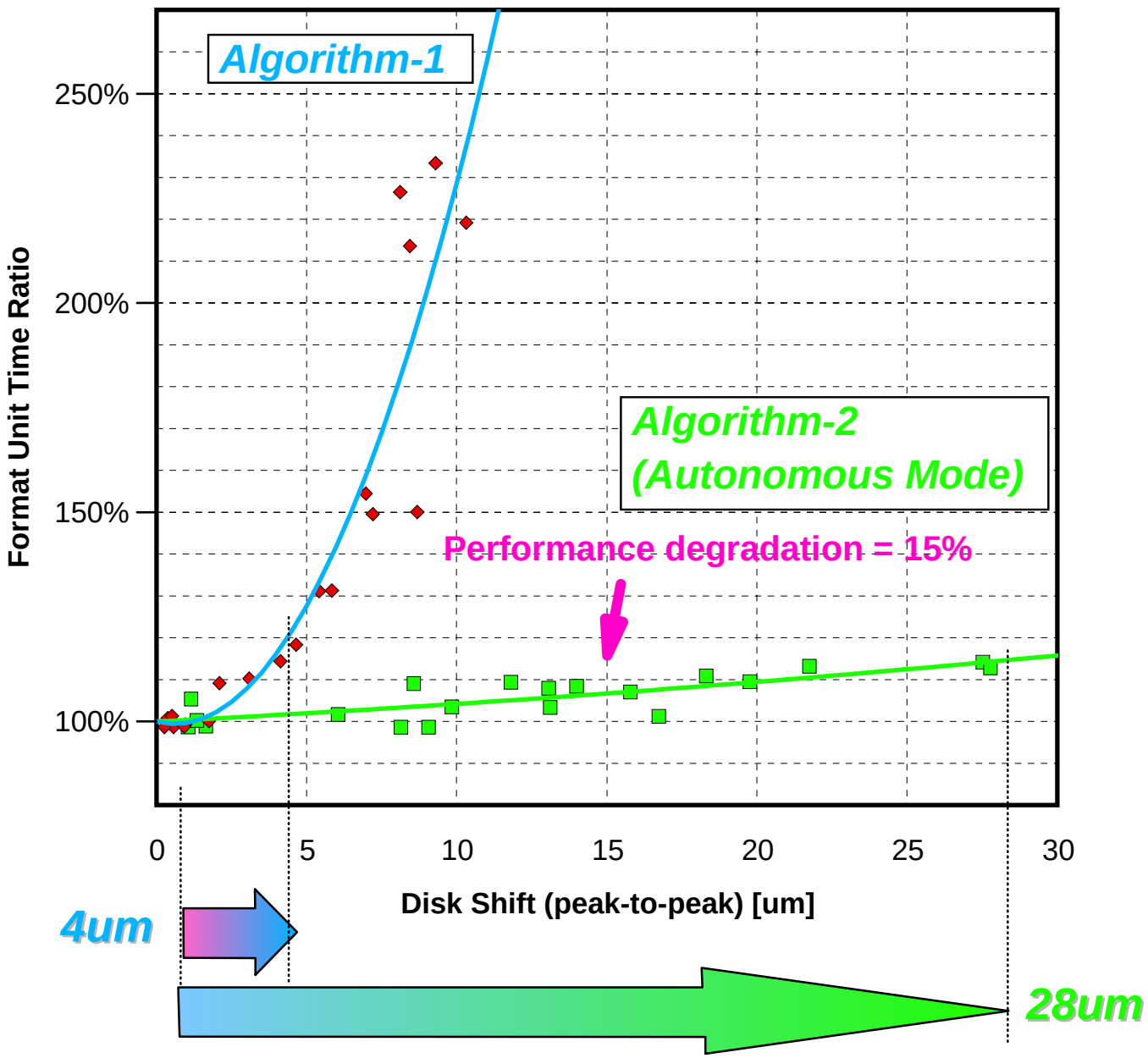
Algorithm-1
Algorithm-2
(Autonomous Mode)
Performance degradation = 15%
Format Unit Time Ratio
250%
200%
150%
100%
0
5
10
15
20
25
30
Disk Shift (peak-to-peak) [um]
4um
28um

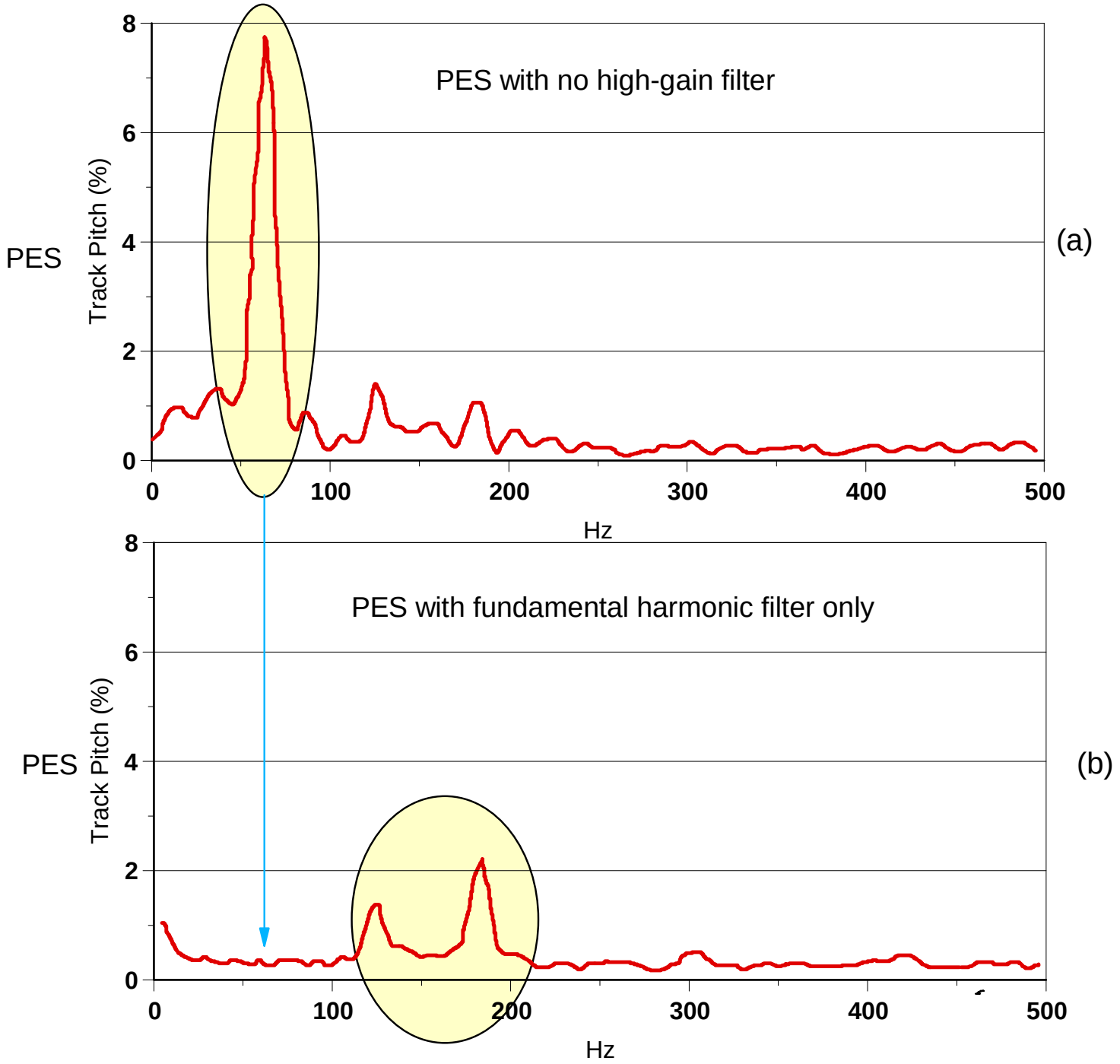
PES with no high-gain filter
PES
Track Pitch (%)
8
6
4
2
0
0
100
200
300
400
500
Hz
(a)
PES with fundamental harmonic filter only
PES
Track Pitch (%)
8
6
4
2
0
0
100
200
300
400
500
Hz
(b)

TrueTrack Servo Solution is Embedded in all Products using a Low Cost LSI Module